PHYSICAL REVIEW A **73**, 011402(R) (2006)

Simultaneous magneto-optical trapping of three atomic species

M. Taglieber,* A.-C. Voigt, F. Henkel, S. Fray, T. W. Hänsch, and K. Dieckmann
Department für Physik der Ludwig-Maximilians-Universität, Schellingstrasse 4, 80799 Munich, Germany and Max-Planck-Institut für Quantenoptik, 85748 Garching, Germany
(Received 3 November 2005; published 24 January 2006)

We report on the simultaneous trapping of two fermionic species, ^{6}Li and ^{40}K, and a bosonic species, ^{87}Rb, demonstrating the first three-species magneto-optical trap ("triple MOT"). The apparatus including the atom sources and the three laser systems is described, and the single-species MOTs and the triple MOT are characterized. In triple MOT operation, typical atom numbers of 3.2×10^7 for ^{6}Li, 1.5×10^7 for ^{40}K, and 5.4×10^9 for ^{87}Rb were achieved. Trap loss due to interspecies collisions was observed. We describe our way to optimize the triple MOT and turn it into a suitable source for the goal to achieve quantum degeneracy by evaporative and sympathetic cooling.

DOI: 10.1103/PhysRevA.73.011402 PACS number(s): 32.80.Pj, 39.25.+k, 03.75.Ss, 34.50.Rk

Following the demonstration of Bose-Einstein condensation in dilute Bose gases [1] and of quantum degeneracy in dilute Fermi gases [2,3], numerous recent experiments focused on the production of ultracold molecules [4,5] using Feshbach resonances. Molecules consisting of two loosely bound fermionic atoms proved to be exceptionally stable against molecular decay [5,6], in contrast to the bosonic case [7]. The demonstration of Bose-Einstein condensation (BEC) of these molecules [3,8], the observation of fermionic condensates of generalized Cooper pairs [9], and their superfluidity [10] marked milestones in the physics of ultracold molecules. However, all these experiments were based on diatomic molecules composed of two fermions of the same species. Ultracold mixtures of two different fermionic atomic species are expected to provide stable systems for the investigation of long-range pairing interactions, for precision spectroscopy of molecules, or for the study of dipolar interaction between heteronuclear diatomic molecules. The first important step in producing a degenerate Fermi gas of two different species is to load the mixture into a magneto-optical trap (MOT). Simultaneous trapping of a bosonic species in addition opens the possibility of sympathetic cooling [11] of the two fermionic species by the bosonic species. So far, two-species magneto-optical traps were realized only for Bose-Bose [12] and for Bose-Fermi [13] mixtures. However, to our knowledge, neither a two-fermion MOT nor a three-species MOT has been demonstrated yet.

In this paper, we report on simultaneous trapping of three species, the fermionic species ^{6}Li and ^{40}K, and the bosonic species ^{87}Rb, using a magneto-optical trap ("triple MOT"). This triple MOT will be used as a precooling stage to obtain the starting conditions for forced evaporative cooling [14] of ^{87}Rb and sympathetic cooling of ^{6}Li and ^{40}K. In the following, we present our experimental system and characterize the optimized triple MOT. With our current setup, we are able to trap 5.4×10^9 ^{87}Rb atoms, 3.2×10^7 ^{6}Li atoms, and 1.5×10^7 ^{40}K atoms simultaneously.

In the experiment, the MOTs for all three species are produced in a steel vacuum chamber ("MOT chamber") at the center of a common magnetic quadrupole field. For loading of the rubidium and potassium MOTs we use atomic vapor dispensers. In order to make loading efficient, these dispensers are placed only 4 cm away from the center of the MOT chamber pointing towards the capture region of the MOTs. This loading configuration does not rely on a sufficient atom mobility on the chamber walls, as it would do in the case of loading from a remote reservoir. The central trapping region of the MOTs is mechanically shaded from the direct atomic flux from the dispensers. For rubidium, we use commercial dispensers (SAES Getters). For potassium, however, dispensers are commercially available with ^{40}K only in the natural abundance of 0.012%. We therefore use home-built dispensers [15] with enriched potassium (3% abundance of ^{40}K). In the case of lithium, vapor loading would be inefficient due to its comparatively low saturation pressure and due to the small fraction of atoms at velocities below a typical capture velocity of the MOT. For this reason, the lithium MOT is loaded from an atomic beam out of a Zeeman slower in spin-flip configuration with a length of 60 cm. The difference between the minimum and the maximum of the magnetic field is set to 810 G, corresponding to a maximum deceleration of the atoms by 761 m/s. The atomic beam is produced by an oven filled with ^{6}Li at almost pure abundance. It is collimated by two tubes of 6 mm diameter and with lengths of 16.5 cm and 13 cm, both located between oven and Zeeman slower. Pumping between the two tubes limits the background gas load from the lithium oven into the MOT chamber.

Figure 1 shows diagrams of the energy levels for the three atomic species together with the transitions used for slowing, trapping, and detection of the atoms. All these transitions are within the respective D_2 lines. The laser systems for lithium, potassium, and rubidium are schematically drawn in Fig. 2. They are based solely on semiconductor laser oscillators and amplifiers, namely grating-stabilized diode lasers (M1–M6), injection-seeded diode lasers (S1–S5) and tapered amplifiers (TA1, TA2). Double pass, quadruple pass, and tandem [18] acousto-optic modulator (AOM) lines are used to shift the frequencies and to control the individual beam powers. Typical AOM frequencies for the MOT operation are indicated in

*Electronic address: matthias.taglieber@mpq.mpg.de

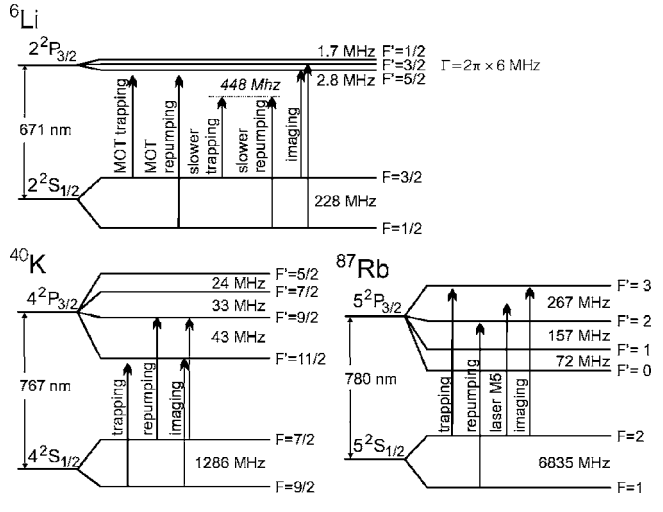

FIG. 1. Atomic energy levels and transitions used to slow and trap lithium, potassium, and rubidium atoms.

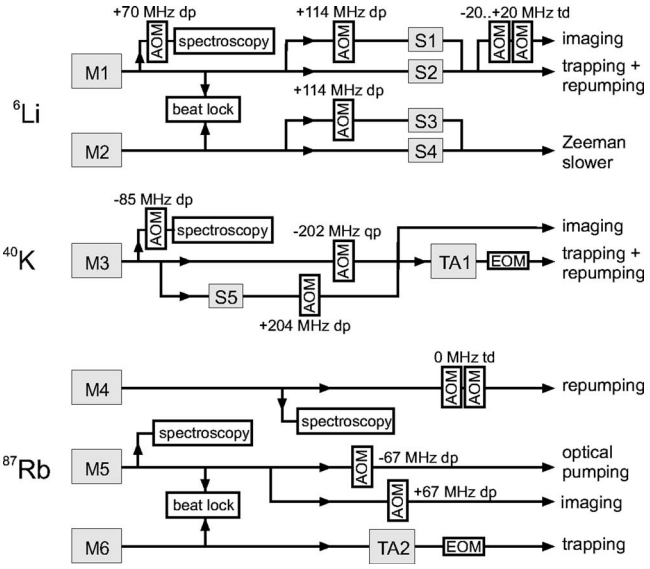

FIG. 2. Laser systems for lithium, potassium, and rubidium. All three laser systems are based on semiconductor lasers. The frequencies are shifted with double pass (dp), quadruple pass (qp), and tandem (td) AOM lines.

the graph. The power in the output beams from the two TAs can be attenuated by means of electro-optical modulators (EOMs).

The different laser locks are implemented as follows: For lithium, the master laser M1 is locked to the $F=1/2, F=3/2 \rightarrow F'$ crossover signal using the side-band free Doppler-free dichroic lock (DFDL) technique [16]. The MOT trapping and repumping light as well as the imaging light are subsequently derived from this laser. The second lithium master laser M2 is referenced to M1 by an offset lock and provides light for the Zeeman slower. For potassium, direct locking to a ^{40}K transition is not favorable due to the very low natural abundance of ^{40}K in the vapor of the spectroscopy cell. Therefore, the master laser M3 is locked to the conveniently located $F=1 \rightarrow F'=0,1,2 - F=2 \rightarrow F'=1,2,3$ crossover signal of the D_2 line of ^{39}K using a standard frequency modulation (FM) locking scheme. Consecutive frequency shifting by means of AOM lines provides all required potassium frequencies. For rubidium, the repumping laser M4 is fixed at the repumping transition by a standard FM lock. The master laser M5 is locked to the $F=2 \rightarrow F'=2,3$ crossover signal with the DFDL technique. Its output is used for imaging and, in the future, for optical pumping. Finally, the rubidium master laser M6 is offset-locked to M5 and provides rubidium trapping light.

All nine resulting laser beams from the three laser systems are sent through individual optical fibers to the MOT setup. The MOT beams are then individually expanded to appropriate intermediate beam waists and combined using edge filters and polarizing beam cubes. The resulting beam containing all three wavelengths is split by polarizing beam splitter cubes into the six arms of the MOT. A telescope in each of the six MOT arms expands the beams to their final $1/e^2$ radii of 7.5 mm for Li, 10 mm for K, and 13 mm for Rb. In order to adjust the intensity balance of the counterpropagating MOT beams simultaneously for all three wavelengths we first use zero-order $\lambda/2$ plates for 780 nm in front of the splitting cubes. This guarantees centering and efficient molasses cooling of the rubidium cloud, while at the same time also centering the potassium cloud. We then adjust the intensity balance of the lithium beams by inserting a stack of two additional $\lambda/2$ plates for the 780 nm wavelength. The two wave plates are mounted together in one rotatable mount with their fast axes aligned. Therefore, the effect of these plates on the polarization of the rubidium light is negligible. The desired splitting ratio of 50% for lithium at the subsequent beam splitter was achieved by careful selection of the plates used in the respective stack. The selection also ensured that the intensity balance for the potassium light is not affected so that all three atomic clouds can be well centered simultaneously.

The atoms are detected with two different methods: fluorescence detection and standard absorption imaging. For the first method the three superimposed MOTs are imaged onto three different photodiodes so that the fluorescence from the different MOTs can be monitored independently. Separation of the fluorescence light originating from the three MOTs is achieved using edge filters and additionally optical band passes. Cross-talk between the three channels is below noise level. The atom numbers derived from the MOT fluorescence signals are calibrated by absorption imaging.

For the realization of the triple MOT we optimized its parameters with the goal to produce an optimally cooled rubidium sample with a large atom number. For future experiments a large rubidium thermal bath for sympathetic cooling of only comparatively small lithium and potassium samples is required. The most obvious constraint imposed on the triple MOT parameters is that for all three species one common magnetic field gradient has to be applied. We therefore started the optimization process by adjusting the laser detunings for maximum atom number of each single-species MOT at several magnetic field gradients. The achievable atom numbers for lithium and potassium were found to be insensitive to the magnetic field gradient over a wide range. For rubidium we found the number of trapped atoms to be high-

TABLE I. Characteristic parameters of the three MOTs: Wavelength and width of the D_2 line, saturation intensity, intensities for trapping and repumping light in each of the six MOT beams, optimized laser detunings, typical atom numbers in single and triple MOT operation, and typical temperature (rubidium molasses temperature in brackets).

	^{6}Li	^{40}K	^{87}Rb
$\lambda_{D_2,\mathrm{vac}}$ (nm)	670.977	766.701	780.241
$\Gamma/2\pi$ (MHz)	5.87	6	6.07
I_{sat} (mW cm^{-2})	2.54	1.80	1.67
$I_{\mathrm{trap}}/I_{\mathrm{sat}}$	0.7	4	8
$I_{\mathrm{repump}}/I_{\mathrm{sat}}$	0.8	1.1	0.5
$\Delta\omega_{\mathrm{trap}}$ (Γ)	−4.3	−4.2	−4.8
$\Delta\omega_{\mathrm{repump}}$ (Γ)	−4.3	0	0
N_{single}	4.2×10^7	2.6×10^7	5.6×10^9
N_{triple}	3.2×10^7	1.5×10^7	5.4×10^9
T (μK)	900	40	800 (50)

est at a magnetic field gradient of 16 G/cm. Table I summarizes the relevant optimized parameters for the single-species MOTs at this magnetic field gradient. In the case of lithium, we were able to trap 4.2×10^7 ^{6}Li atoms at an initial loading rate of 1×10^8 s^{-1} in the single-species MOT using a detuning of $-4.3\Gamma_{\mathrm{Li}}$ for the repumping and trapping light. The average peak intensity per beam was 0.7 and 0.8 times the saturation intensity I_{sat} of the respective transition. In the potassium MOT the peak intensities of the trapping and repumping light were 4 I_{sat} and 1.1 I_{sat}, respectively. The highest atom number of 2.6×10^7 ^{40}K atoms and an initial loading rate of 5×10^7 s^{-1} in single-species MOT operation were achieved at a detuning of $-4.2\Gamma_{\mathrm{K}}$ for the trapping light and with resonant repumping light. For the rubidium MOT we used average peak intensities of 8 I_{sat} for the trapping light and 0.5 I_{sat} for the repumping light. In the single-species case we found a maximum atom number of $N_{\mathrm{Rb}}=5.6\times10^9$ atoms and an initial loading rate of 8×10^9 s^{-1} for resonant repumping light and a detuning of $-4.8\Gamma_{\mathrm{Rb}}$ for the trapping light.

In triple MOT operation, atom numbers of 3.2×10^7 ^{6}Li, 1.5×10^7 ^{40}K, and 5.4×10^9 ^{87}Rb were simultaneously trapped. In comparison to single MOT operation, this corresponds to a reduction of the steady state atom numbers of the lithium and potassium MOTs by 24% and 42%, respectively. For the rubidium MOT, however, no significant reduction was observed.

Figure 3 depicts a typical time evolution of the atom numbers as inferred from the fluorescence signals for a particular sequence used to study the triple MOT. It shows the simultaneous trapping of the three species in the triple MOT and illustrates the influences between the different species. During the whole sequence, the trapping light for all three species and the comparatively strong repumping light for lithium were kept switched on. At times $t<0$ however, loading of the lithium MOT was avoided by a mechanical shutter blocking the lithium atom beam in front of the Zeeman slower. Loading and trapping of potassium and rubidium

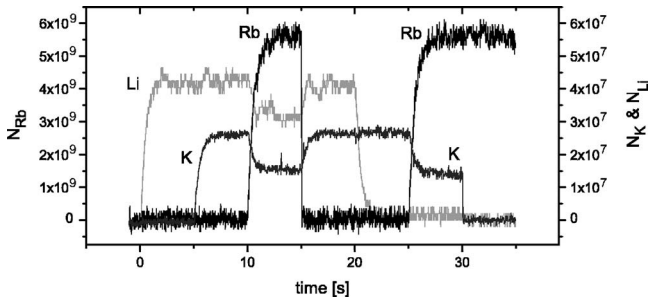

FIG. 3. Typical loading sequence of the Li+K+Rb triple MOT. Trapping of Rb and K is controlled by switching the corresponding repumping beam on or off. In the case of Li the atomic loading beam from the Zeeman slower is blocked and unblocked by a mechanical shutter. The atom numbers are monitored by calibrated fluorescence detection.

were suppressed by switching off the corresponding repumping light. At $t=0$ the lithium atom beam shutter was opened and the lithium MOT loaded to its steady state atom number for single-species MOT operation. After 5 s the potassium repumping light was switched on and the potassium MOT loaded to its steady state atom number. We could not observe any decrease in the lithium atom number due to the presence of a potassium MOT in any of our measurements. The same holds true for the potassium MOT in the presence of a lithium MOT. However, when the rubidium repumping light was switched on at $t=10$ s, the lithium and potassium atom numbers decreased to the steady state values for triple MOT operation within one second. At $t=15$ s, the rubidium repumping light was switched off again. The lithium and the potassium MOTs then both regained their initial single-species steady state atom numbers on a time scale typical for their loading in the single-species MOT operation. The remaining part of this particular sequence illustrates that no significant reduction of atom number in the rubidium MOT due to the presence of the potassium MOT could be observed.

We attribute the decrease of the steady state atom numbers in triple MOT operation compared to single MOT operation to additional losses in the MOTs due to collisions between trapped lithium and rubidium atoms and between trapped potassium and rubidium atoms. We therefore studied these losses in the two-species MOTs Li+Rb and K+Rb. The rate equation for the potassium atom number in a K+Rb two-species MOT is given by

$$\frac{dN_{\mathrm{K}}}{dt} = L_{\mathrm{K}} - \gamma_{\mathrm{K}} N_{\mathrm{K}} - \beta_{\mathrm{K}} \int n_{\mathrm{K}}^2 dV - \beta_{\mathrm{K,Rb}} \int n_{\mathrm{K}} n_{\mathrm{Rb}} dV,$$

where L_{K} is the loading rate and γ_{K} is the coefficient for losses due to collisions with the background gas. The third term accounts for losses due to collisions between two different trapped potassium atoms and the last term reflects losses due to interspecies collisions of trapped atoms. Because of the comparatively low potassium atom number, the losses due to intraspecies collisions can be neglected when compared to the two other loss terms. The interspecies loss coefficient $\beta_{\mathrm{K,Rb}}$ is then easily obtained from the potassium

loading rate, the steady state atom numbers N_K^∞ and $N_K^{\infty\prime}$ in single and double MOT operation, and the peak density $n_{Rb}^{(0)}=1.4\times10^{11}$ cm^{-3} of the rubidium MOT. Under the assumption that the atomic clouds have Gaussian shapes it is given by $\beta_{K,Rb}=(L_K/n_{Rb}^{(0)}\kappa)[(1/N_K^{\infty\prime})-(1/N_K^\infty)]$. In this equation, κ is a factor of the order 1 that accounts for the different waists of the potassium and rubidium atom clouds. The rubidium peak density and κ are obtained from absorption imaging whereas all other values are extracted from the calibrated potassium MOT fluorescence monitor signal. Our experimental data for the K+Rb double MOT and analogous measurements for the Li+Rb double MOT yield $\beta_{K,Rb}=1\times10^{-11}$ cm^3 s^{-1} and $\beta_{Li,Rb}=8\times10^{-12}$ cm^3 s^{-1}, which gives the order of magnitude of these loss coefficients.

A second important parameter for future experiments is the temperature of the atomic clouds. Therefore the temperatures of the MOTs in single and triple MOT operation were measured. We found them to be identical within measurement accuracy. Typical MOT temperatures were on the order of 900 μK for lithium, 40 μK for potassium, and 800 μK for rubidium. The temperature of the rubidium cloud could be reduced to a minimum of 50 μK after only 2 ms of molasses cooling. The potassium temperature could not significantly be lowered by molasses. In the case of lithium, a molasses phase led to heating. The short time needed for molasses cooling of rubidium is therefore an important result for the application of the triple MOT, since the lithium and potassium clouds will have to expand freely during the rubidium molasses before they can be recaptured in a magnetic trap.

In summary, we have demonstrated simultaneous trapping of fermionic ^{6}Li and ^{40}K and bosonic ^{87}Rb in a three-species MOT. We have presented the apparatus including the Zeeman slower and the laser systems by which we were able to simultaneously confine 3.2×10^7 ^{6}Li atoms, 1.5×10^7 ^{40}K atoms, and 5.4×10^9 ^{87}Rb atoms. This triple MOT is a suitable source of precooled atoms for magnetic transport [17] into an UHV chamber and subsequent evaporative and sympathetic cooling into quantum degeneracy.

[1] M. H. Anderson *et al.*, Science **269**, 198 (1995); C. C. Bradley *et al.*, Phys. Rev. Lett. **75**, 1687 (1995); K. B. Davis *et al.*, *ibid.* **75**, 3969 (1995); C. C. Bradley, C. A. Sackett, and R. G. Hulet, *ibid.* **78**, 985 (1997).

[2] B. DeMarco and D. S. Jin, Science **285**, 1703 (1999); A. G. Truscott *et al.*, *ibid.* **291**, 2570 (2001); F. Schreck *et al.*, Phys. Rev. Lett. **87**, 080403 (2001); S. R. Granade *et al.*, *ibid.* **88**, 120405 (2002); Z. Hadzibabic *et al.*, *ibid.* **88**, 160401 (2002);.

[3] S. Jochim *et al.*, Science **302**, 2101 (2003).

[4] E. A. Donley *et al.*, Nature (London) **417**, 529 (2002); C. A. Regal *et al.*, *ibid.* **424**, 47 (2003).

[5] K. E. Strecker, G. B. Partridge, and R. G. Hulet, Phys. Rev. Lett. **91**, 080406 (2003); J. Cubizolles *et al.*, *ibid.* **91**, 240401 (2003); S. Jochim *et al.*, *ibid.* **91**, 240402 (2003);.

[6] C. A. Regal, M. Greiner, and D. S. Jin, Phys. Rev. Lett. **92**, 083201 (2004).

[7] S. Inouye *et al.*, Nature (London) **392**, 151 (1998).

[8] M. Greiner, C. A. Regal, and D. S. Jin, Nature (London) **426**, 537 (2003); M. W. Zwierlein *et al.*, Phys. Rev. Lett. **91**, 250401 (2003).

[9] C. A. Regal, M. Greiner, and D. S. Jin, Phys. Rev. Lett. **92**, 040403 (2004); M. W. Zwierlein *et al.*, *ibid.* **92**, 120403 (2004).

[10] M. W. Zwierlein *et al.*, Nature (London) **435**, 1047 (2005).

[11] D. J. Wineland, R. E. Drullinger, and F. L. Walls, Phys. Rev. Lett. **40**, 1639 (1978); D. J. Larson *et al.*, *ibid.* **57**, 70 (1986); C. J. Myatt *et al.*, *ibid.* **78**, 586 (1997).

[12] W. Süptitz *et al.*, Opt. Lett. **19**, 1571 (1994); M. S. Santos *et al.*, Phys. Rev. A **52**, R4340 (1995); G. D. Telles *et al.*, *ibid.* **59**, R23 (1999); G. D. Telles *et al.*, *ibid.* **63**, 033406 (2001); U. Schlöder *et al.*, Eur. Phys. J. D **7**, 331 (1999); V. Wippel, C. Binder, and L. Windholz, *ibid.* **21**, 101 (2002); C. I. Sukenik and H. C. Busch, Phys. Rev. A **66**, 051402 (2002); S. Hensler *et al.*, J. Mod. Opt. **51**, 1807 (2004).

[13] M. O. Mewes *et al.*, Phys. Rev. A **61**, 011403(R) (1999); J. Goldwin *et al.*, *ibid.* **65**, 021402(R) (2002).

[14] N. Masuhara *et al.*, Phys. Rev. Lett. **61**, 935 (1988).

[15] B. DeMarco, H. Rohner, and D. S. Jin, Rev. Sci. Instrum. **70**, 1967 (1999).

[16] G. Wasik *et al.*, Appl. Phys. B **75**, 613 (2002).

[17] M. Greiner *et al.*, Phys. Rev. A **63**, 031401(R) (2001).

[18] Technical note: A tandem AOM line consists of two consecutive AOMs with frequencies $\nu_0-\delta/2$ and $-\nu_0-\delta/2$ allowing a frequency tuning by typically $\delta=-20\ldots+20$ MHz with constant beam pointing.